

# Coronavirus Disease 2019 (COVID-19) CT Findings: A Systematic Review and Meta-analysis

Q1 Q3 Cuiping Bao, Xuehuan Liu, Han Zhang, Yiming Li, MD, PhD, Jun Liu, MD, PhD

## Abstract

**Purpose:** To date, considerable knowledge gaps remain regarding the chest CT imaging features of COVID-19. We performed a systematic review and meta-analysis of results from published studies to date to provide a summary of evidence on detection of COVID-19 by chest CT and the expected CT imaging manifestations.

**Methods:** Studies were identified by searching PubMed database for articles published between December 2019 and February 2020. Pooled CT positive rate of COVID-19 and pooled incidence of CT imaging findings were estimated using a random-effect model.

**Results:** A total of 13 studies met inclusion criteria. The pooled positive rate of the CT imaging was 89.76% and 90.35% when only including thin-section chest CT. Typical CT signs were ground glass opacities (83.31%), ground glass opacities with mixed consolidation (58.42%), adjacent pleura thickening (52.46%), interlobular septal thickening (48.46%), and air bronchograms (46.46%). Other CT signs included crazy paving pattern (14.81%), pleural effusion (5.88%), bronchiectasis (5.42%), pericardial effusion (4.55%), and lymphadenopathy (3.38%). The most anatomic distributions were bilateral lung infection (78.2%) and peripheral distribution (76.95%). The incidences were highest in the right lower lobe (87.21%), left lower lobe (81.41%), and bilateral lower lobes (65.22%). The right upper lobe (65.22%), right middle lobe (54.95%), and left upper lobe (69.43%) were also commonly involved. The incidence of bilateral upper lobes was 60.87%. A considerable proportion of patients had three or more lobes involved (70.81%).

**Conclusions:** The detection of COVID-19 chest CT imaging is very high among symptomatic individuals at high risk, especially using thin-section chest CT. The most common CT features in patients affected by COVID-19 included ground glass opacities and consolidation involving the bilateral lungs in a peripheral distribution.

**Key Words:** CT imaging findings, COVID-19, ground glass opacities, meta-analysis, thin-section chest CT

J Am Coll Radiol 2020; ■:■-■. Copyright © 2020 American College of Radiology

## INTRODUCTION

Beginning in December 2019, a number of cases with pneumonia of unexplained cause occurred in Wuhan, Hubei province, China. Deep sequencing from lower respiratory tract samples confirmed infection was caused by a novel coronavirus that had previously not been found in humans or animals. Subsequently, this novel coronavirus was named corona virus disease 2019 (COVID-19) by the World Health Organization [1]. COVID-19 infection

causes clusters of severe respiratory illness, and its main clinical manifestations are fever, cough, shortness of breath, and myalgia or fatigue [2,3]. Not only patients with symptoms but also patients in the incubation period can become the source of infection. Therefore, early diagnosis is very important.

Radiological examination, as a routine imaging tool for pneumonia diagnosis, is of great importance in the early detection and treatment of patients affected by COVID-19. Radiological examinations are relatively easy to perform and can produce fast diagnosis. Chest radiography is not sensitive for the detection of ground-glass opacity (GGO) and may demonstrate normal findings in early stage of infection. In contrast, thin-section chest CT examination plays a key role in assisting diagnosis. To date, considerable knowledge gaps remain in the chest CT imaging features of COVID-19.

In this systematic review and meta-analysis, we aim to quantitatively summarize results from published studies to

Department of Radiology, Tianjin Union Medical Center, Tianjin, China. Corresponding authors and reprints: Yiming Li, MD, PhD, Department of Radiology, Tianjin Union Medical Center, 190 Jieyuan Road, Hongqiao District, Tianjin 300121, PR China.\*\*Jun Liu, MD, PhD, Department of Radiology, Tianjin Union Medical Center, 190 Jieyuan Road, Hongqiao District, Tianjin 300121, PR China.e-mail: [riminglee@126.com](mailto:riminglee@126.com) or [cjr.liujun@vip.163.com](mailto:cjr.liujun@vip.163.com).

The authors state that they have no conflict of interest related to the material discussed in this article.

107 date to provide a more precise estimate of detection of  
108 COVID-19 by chest CT and report on the most common  
109 imaging findings on chest CT imaging.  
110

## 111 MATERIALS AND METHODS

### 112 Retrieval of Studies

113 We searched PubMed for studies reporting CT imaging  
114 features of COVID-19 published between December 1,  
115 2019, and February 29, 2020. The search terms included  
116 (COVID-19) OR (2019 Novel Coronavirus) OR (2019-  
117 nCoV). In addition, we reviewed the reference lists of  
118 retrieved articles for additional articles. Two independent  
119 investigators screened titles or abstracts according to the  
120 inclusion and exclusion criteria. The meta-analysis was  
121 performed using Preferred Reporting Items for Systematic  
122 Reviews and Meta-Analyses guidelines.  
123

### 124 Inclusion and Exclusion Criteria

125 Titles and abstracts of the articles were screened using the  
126 following inclusion criteria to identify all eligible studies: (1)  
127 publications were original articles with full text; (2) the  
128 mean or median age of the study population was above 18  
129 years; (3) at least one of the outcomes was chest CT imaging  
130 features of COVID-19; (4) the number of patients with  
131 corresponding imaging features was reported in the study.  
132 Studies were excluded if they (1) lacked corresponding  
133 outcome parameters or research data or (2) did not have  
134  
135

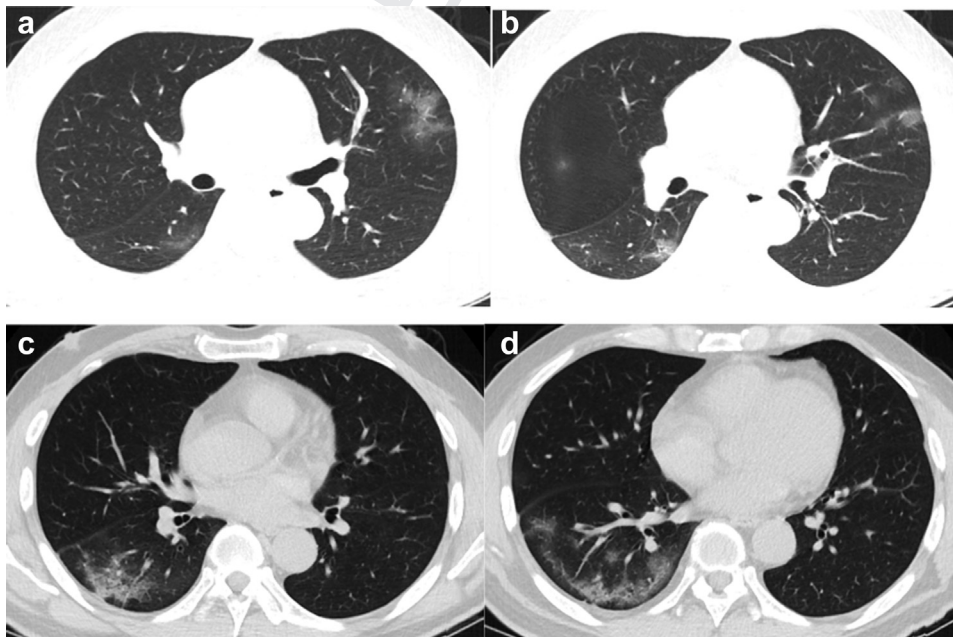
136 available full texts. When there were multiple publications  
137 from the same population, only data from the most recent  
138 report or the study with the larger sample size was included.  
139

### 140 Data Extraction

141 We extracted the following information from each publi-  
142 cation: the first author's full name, study sample size, mean  
143 or median age, gender distribution, application of thin-  
144 section chest CT, results of chest CT imaging features,  
145 and number of patients with each corresponding imaging  
146 features. The recorded chest CT imaging features mainly  
147 included the following aspects: (1) patterns of the lesion  
148 (GGO, consolidation, GGO mixed consolidation, air  
149 bronchogram, interlobular septal thickening, crazy paving  
150 pattern, bronchiectasis, adjacent pleura thickening, pleural  
151 effusion, pericardial effusion, lymphadenopathy), (2) lesion  
152 distribution (bilateral lung, peripheral, central), and (3) lobe  
153 distribution and the number of lobes involved (Fig. 1).  
154

### 155 Statistical Analysis

156 In this systematic review and meta-analysis, we pooled data  
157 using single-arm analysis. Because some proportions  
158 extracted from the original data were too high or too low, we  
159 transformed the data using the double arcsine method into a  
160 normal distribution. We conducted the meta-analysis using  
161 the transformed data. The pooled proportion was calculated  
162 using the result of the meta-analysis by the formula  
163  
164  
165  
166  
167  
168  
169  
170  
171  
172  
173  
174  
175  
176  
177  
178  
179  
180  
181  
182  
183  
184  
185  
186  
187  
188  
189  
190  
191  
192  
193  
194  
195  
196  
197  
198  
199  
200  
201  
202  
203  
204  
205  
206  
207



208 **Fig 1.** Baseline CT images (a-d) of a 50 year-old man admitted for symptoms of fever for 1 day: there were multiple patchy  
209 ground-glass opacities in the left upper lobe and right lower lobe (a, b). Air bronchogram and crazy paving pattern can be  
210 seen (c). Lesions are located in the peripheral area of the lung (d).

( $P = (\sin(tp/2))^2$ ). Statistical heterogeneity between studies was evaluated with Cochran's  $Q$  test and the  $I^2$  statistic [4]. For the  $Q$  statistic, a  $P$  value  $< .10$  was considered statistically significant for heterogeneity; for  $I^2$ , a value  $>50\%$  was considered to have severe heterogeneity. Publication bias was evaluated by constructing a funnel plot and by Egger's test [5]. For Egger's test, a  $P$  value  $< .10$  was considered statistically significant. All statistical analyses were performed with Stata SE 13 for Windows.

## RESULTS

### Characteristics of the Subjects in Selected Studies

Detailed search procedures are summarized in Figure 2. All of the full texts of the 41 identified articles were retrieved for detailed evaluation. Of them, 28 articles did not meet the inclusion criteria, including 6 duplicated populations, 15 case reports or case series, 3 without related data, and 4 review articles. The remaining 13 independent studies were used in the current analysis [6-18] (Table 1). Of these studies, 10 studies reported one or more chest CT imaging signs [6-8,10-12,14-16,18], 11 studies reported at least one kind of lung distribution [6-8,10,11,13-18], and 5 studies reported the lobes and total number of lobes involved [7,9,11,15,16].

The 13 studies had 2,738 participants with 2,386 having abnormal CT imaging features. In the primary meta-analysis, we found that the pooled positive rate of the CT imaging was 89.76% (95% confidence interval [CI]: 84.42%-93.84%) (Fig. 3). When we excluded the studies without mention of thin-section chest CT, the result was 90.35% (95%CI: 83.68%-95.42%) (Fig. 4).

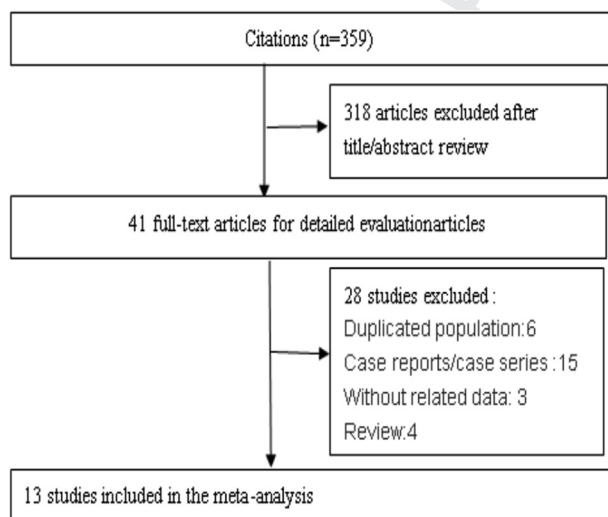


Fig 2. Flowchart on the article selection process.

### Patterns of the Lesion

In this meta-analysis, we found that typical CT imaging appearance for COVID-19 patients was GGO. The incidence of GGO was 83.31% (95% CI: 69.43%-93.35%). When we excluded the studies without mention of thin-section chest CT, the incidence of GGO was 85.49% (95% CI: 64.74%-97.89%). The incidence of GGO with mixed consolidation was 58.42% (95% CI: 48.46%-67.58%). The incidences of interlobular septal thickening, adjacent pleura thickening, and air bronchogram were also high: 48.46% (95% CI: 11.44%-86.19%), 52.46% (95% CI: 15.53%-87.54%), and 46.46% (95% CI: 17.76%-76.95%), respectively. The incidence of crazy paving pattern was 14.81% (95% CI: 6.61%-25.99%). Other atypical CT imaging findings included bronchiectasis (5.42%, 95% CI: 0.02%-19.31%), pleural effusion (5.88%, 95% CI: 3.38%-8.73%), pericardial effusion (4.55%, 95% CI: 2.09%-7.90%), and lymphadenopathy (3.38%, 95% CI: 1.00%-6.86%), respectively (Table 2).

### Lesion Distribution

We found that most patients with COVID-19 have bilateral lung infection; the incidence was 78.2% (95% CI: 65.69%-88.19%). When we excluded the studies without mention of thin-section chest CT, bilateral lung infection was seen in 81.80% of patients (95% CI: 73.94%-88.51%). The lesions were mostly located in the peripheral area (76.95%, 95% CI: 57.43%-91.50%). Fewer lesions were located in the central (peribronchovascular) area (10.81%, 95% CI: 0.12%-41.50%) (Table 2).

### Lobe Distribution and Number of Lobes Involved

COVID-19 infection can involve all lobes. In this pooled meta-analysis, we found that the right lower lobe and left lower lobe were the most commonly involved; 87.21% (95% CI: 80.23%-92.84%) and 81.41% (95% CI: 76.1%-86.53%), respectively. The incidence of bilateral lower lobes was 65.22% (95% CI: 55.95%-73.94%). The right upper lobe and left upper lobe were also commonly involved: 65.22% (95% CI: 54.95%-75.24%) and 69.43% (95% CI: 58.91%-79.02%), respectively. The incidence of bilateral upper lobes was 60.87% (95% CI: 51.46%-69.43%). More than half patients had right middle lobe infection (54.95%, 95% CI: 47.96%-61.36%). There were 39.54% (95% CI: 33.76%-45.96%) of patients with all lobes affected and 20.51% (95% CI: 13.76%-28.22%) patients with four lobes affected. A significant proportion of patients had three or more lobes involved (70.81%, 95% CI: 61.75%-79.10%) (Table 2).

Table 1. Characteristics of 13 reviewed studies

Study	Sample Size	Mean or Median Age	Gender	Thin-section Chest CT	CT Abnormal	CT Imaging Manifestations
Zhang et al [18]	9	35	Male: 5 Female: 4	Yes	7	GGO, consolidation, bilateral lung Pleural effusion
Song et al [11]	51	49	Male: 25 Female: 26	Yes	51	GGO, consolidation, bilateral lung, peripheral, central, pleural effusion, pericardial effusion, lymphadenopathy
Pan et al [9]	63	44.9	Male: 33 Female: 30	Yes	63	GGO, consolidation
Wu et al	80	44	Male: 42 Female: 38	Yes	76	GGO, consolidation, interlobular septal thickening, crazy paving pattern, pleural effusion, pericardial effusion, lymphadenopathy, peripheral, central
Bernheim et al [7]	121	45.3	Male: 61 Female: 60	Yes (22 with conventional CT)	94	GGO, consolidation, crazy paving pattern, pleural effusion, bronchiectasis, lymphadenopathy, peripheral, central
Ai et al [6].	1,014	51	Male: 467 Female: 547	Yes	888	Bilateral lung, GGO, consolidation, interlobular septal thickening
Shi et al [10]	81	49.5	Male: 42 Female: 39	Yes	81	Bilateral lung, GGO, consolidation, interlobular septal thickening, adjacent pleura thickening, air bronchogram, pleural effusion, bronchiectasis, lymphadenopathy, peripheral
Wang et al [12]	52	44	Male: 29 Female: 23	Yes	50	GGO, consolidation, interlobular septal thickening
Xu et al [16]	50	43.9	Male: 29 Female: 21	Yes	41	GGO, consolidation, interlobular septal thickening, air bronchogram, pleural effusion, peripheral, central

(continued)

Table 1. Continued

Study	Sample Size	Mean or Median Age	Gender	Thin-section Chest CT	CT Abnormal	CT Imaging Manifestations
Zhang et al [17]	140 (135 with chest CT scan)	57	Male: 69 Female: 71	Without mention	134	Bilateral lung
Guan et al [8]	1,099 (975 with chest CT scan)	47	Male: 637 Female: 459	Without mention	840	Bilateral lung, GGO, interlobular septal thickening,
Wu et al	80	46.1	Male: 39 Female: 41	Without mention	55	Bilateral lung
Xu et al [15]	90	50	Male: 39 Female: 51	Yes	69	Bilateral lung, GGO, consolidation, crazy paving pattern, interlobular septal thickening, air bronchogram, adjacent pleura thickening, pleural effusion, pericardial effusion, lymphadenopathy, peripheral

GGO = ground-glass opacities.

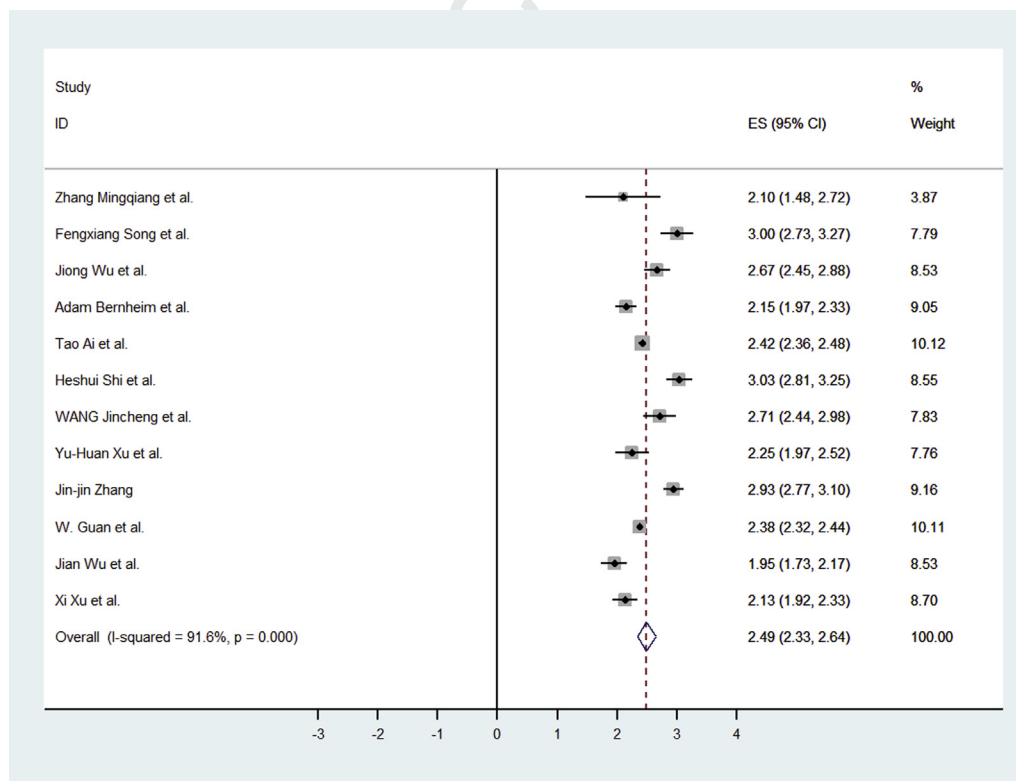


Fig 3. Forest plot of the studies for abnormal CT among presumed coronavirus disease 2019 infection. CI = confidence interval; ES.

print & web 4C/FPO

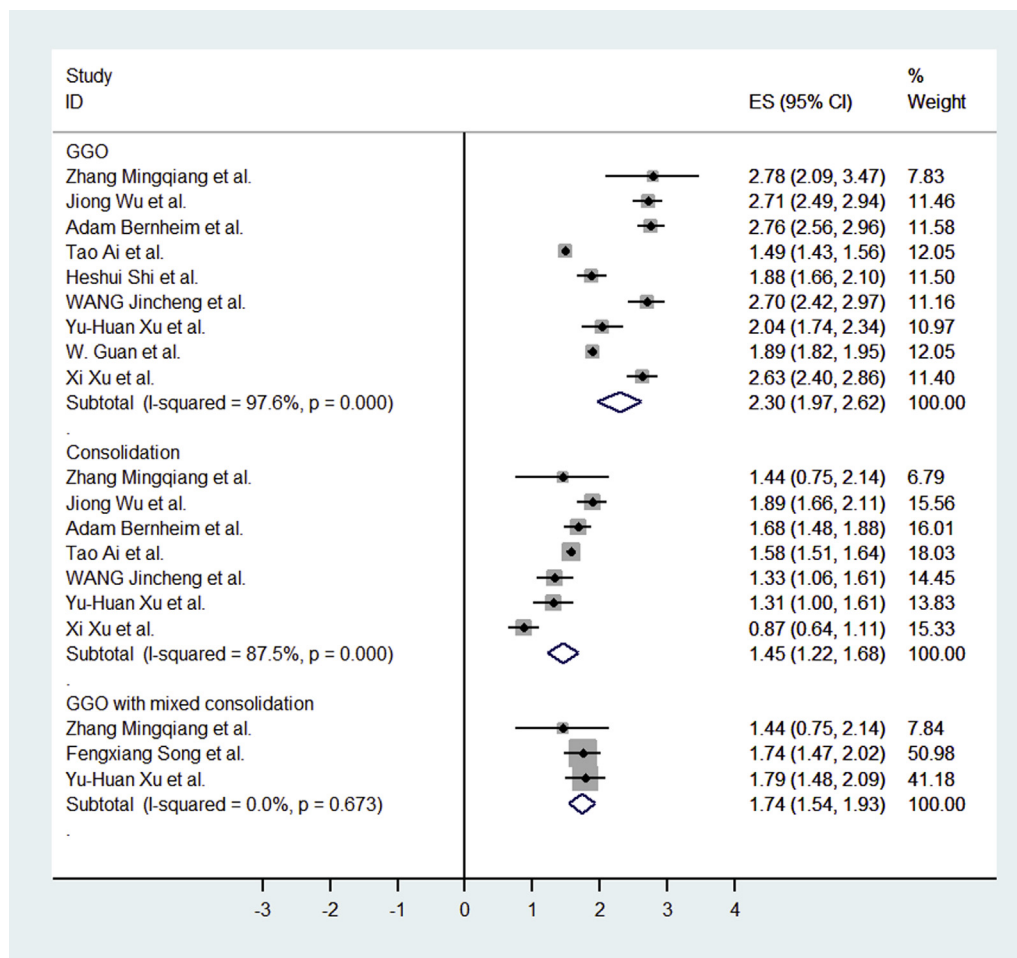


Fig 4. Forest plot of the studies for CT findings (GGO, consolidation, GGO with mixed consolidation). CI = confidence interval; ES; GGO = ground-glass opacities.

## Publication Bias

*P* values for Egger's regression asymmetry test are shown in Table 3. There was a low probability of publication bias in the following subgroups: GGO mixed consolidation, air bronchogram, crazy paving pattern, pleural effusion, pericardial effusion, lymphadenopathy, peripheral, lobe of lesion distribution, and number of lobes involved. However, there was publication bias in the subgroup of abnormal GGO, consolidation, and bilateral lung involvement. Because there were only two studies in the subgroup of bronchiectasis, adjacent pleura thickening, central and bilateral upper lobes, and bilateral lower lobes, the publication bias could not be evaluated.

## DISCUSSION

Our systematic review and meta-analysis suggests that the proportion of COVID-19 detected by chest CT imaging is very high. The most typical CT imaging finding is GGO.

Other common CT features in patients affected by COVID-19 included consolidation, interlobular septal thickening, adjacent pleura thickening, and air bronchograms. More than half of the patients manifested as GGO, consolidation, and adjacent pleura thickening. Imaging findings mostly involved the bilateral lungs and were located in the peripheral area of the lungs. The infection can involve all the lobes and mostly the bilateral lower lobes.

Some patients who had negative reverse-transcription polymerase chain reaction for COVID-19 at initial presentation may still show chest CT abnormalities [19]. Fang et al reported that the sensitivity of first reverse-transcription polymerase chain reaction is 71%, which may be lower than that of chest CT [20]. In our meta-analysis of 2,738 cases, the pooled positive rate of CT imaging was 89.76% among patients suspected to have COVID-19. Thus, chest CT plays an important role in the early diagnosis of COVID-19.

In this analysis, we found that the typical CT features of COVID-19 are GGO and lung consolidation. Some of the

Table 2. CT imaging findings in the meta-analysis

CT Manifestations	Pooled Transformed Results (95% CI)	Pooled Proportion (95% CI)*
Patterns of the lesion		
GGO	2.3 (1.97-2.62)	83.31 (69.43-93.35)
Consolidation	1.45 (1.22-1.68)	43.97 (32.82-55.45)
GGO mixed consolidation	1.74 (1.54-1.93)	58.42 (48.46-67.58)
Air bronchogram	1.5 (0.87-2.14)	46.46 (17.76-76.95)
Interlobular septal thickening	1.54 (0.69-2.38)	48.46 (11.44-86.19)
Crazy paving pattern	0.79 (0.52-1.07)	14.81 (6.61-25.99)
Bronchiectasis	0.47 (0.03-0.91)	5.42 (0.02-19.31)
Adjacent pleura thickening	1.62 (0.81-2.42)	52.46 (15.53-87.54)
Pleural effusion	0.49 (0.37-0.6)	5.88 (3.38-8.73)
Pericardial effusion	0.43 (0.29-0.57)	4.55 (2.09-7.90)
Lymphadenopathy	0.37 (0.2-0.53)	3.38 (1.00-6.86)
Lesion distribution		
Bilateral lung	2.17 (1.89-2.44)	78.2 (65.69-88.19)
Peripheral	2.14 (1.72-2.55)	76.95 (57.43-91.50)
central	0.67 (-0.07-1.4)	10.81 (0.12-41.50)
Lobe of lesion distribution		
Right upper lobe	1.88 (1.67-2.1)	65.22 (54.95-75.24)
Right middle lobe	1.67 (1.53-1.8)	54.95 (47.96-61.36)
Right lower lobe	2.41 (2.22-2.6)	87.21 (80.23-92.84)
Left upper lobe	1.97 (1.75-2.19)	69.43 (58.91-79.02)
Left lower lobe	2.25 (2.12-2.39)	81.41 (76.1-86.53)
Bilateral upper lobes	1.79 (1.6-1.97)	60.87 (51.46-69.43)
Bilateral lower lobes	1.88 (1.69-2.07)	65.22 (55.95-73.94)
Number of lobes involved		
1	0.81 (0.52-1.09)	15.53 (6.61-26.88)
2	0.75 (0.62-0.87)	13.42 (9.31-17.76)
3	0.67 (0.55-0.8)	10.81 (7.37-15.16)
4	0.94 (0.76-1.12)	20.51 (13.76-28.22)
5	1.36 (1.24-1.49)	39.54 (33.76-45.96)
Lobes involved $\geq 3$	2 (1.808-2.192)	70.81 (61.75-79.10)

CI = confidence interval; GGO = ground glass opacities.

\*The results are expressed as a percentage.

GGO were further developed into reticular interlobular septa thickening and crazy paving pattern, indicating that the infection leads to diffuse alveolar edema and interstitial inflammation [21,22]. Several patients seemed to have pleural effusion, which may represent a poor prognostic indicator [23]. Generally, viral pneumonias have similar etiological mechanisms and typical imaging findings of COVID-19. Thus, these findings also appear in other viral pneumonia such as the common cold, influenza, and other coronaviruses diseases including severe acute respiratory syndrome and Middle East respiratory syndrome [24-28].

Because COVID-19, severe acute respiratory syndrome, and Middle East respiratory syndrome all belong to the family of coronaviruses, the CT imaging signs are more similar. Still, there seems to be unique imaging characteristics for COVID-19. Unilateral involvement is more common in the early stage of severe acute respiratory syndrome and Middle East respiratory syndrome [29,30]. In contrast, COVID-19 infection seems to be more commonly bilateral. In this meta-analysis, most patients had bilateral lung involvement, especially the bilateral lower lobes. Overall, 70% of patients had three or more lobes involved.

Table 3. Results of the Egger test

CT Manifestations	P	Lobe of Lesion Distribution	P
Abnormal CT	<.001	Right upper lobe	.264
GGO	.001	Right middle lobe	.142
Consolidation	.007	Right lower lobe	.074
GGO mixed consolidation	.116	Left upper lobe	.056
Air bronchogram	.974	Left lower lobe	.064
Interlobular septal thickening	.025	Bilateral upper lobes	NA
Crazy paving pattern	.456	Bilateral lower lobes	NA
Bronchiectasis	NA	Number of lobes involved	
Adjacent pleura thickening	NA	1	.379
Pleural effusion	.675	2	.189
Pericardial effusion	.942	3	.219
Lymphadenopathy	.716	4	.563
Lesion distribution		5	.067
Bilateral lung	<.001	Lobes involved $\geq 3$	.131
Peripheral	.890		
Central			

GGO = ground glass opacities; NA = the publication bias could not be tested.

Our meta-analysis has several strengths. First, the number of cases included was relatively large for 3 months of early publications, providing aggregate evidence for evaluating diagnosis of COVID-19 by chest CT. Second, the included studies were conducted in different hospitals and settings, making the results more generalizable. Third, in this analysis, we extract varieties of different imaging features, including both specific imaging features and distribution patterns in the lungs.

Our meta-analysis also has several limitations. First a majority of the studies included did not distinguish between clinically mild, moderate, and severe patients. Furthermore, some patients may have comorbidities and chronic diseases such as diabetes and hypertension that we cannot account for. These factors may affect imaging appearances. Second, due to different CT scanners and interpreting radiologists, the reported imaging features may be variable across sites.

### TAKE-HOME POINTS

- Our systematic review and meta-analysis of the early literature suggests that the proportion of suspected COVID-19 detected by chest CT imaging is high.
- Chest CT, especially thin-section chest CT, can play a central role in early diagnosis of COVID-19.

- The most common CT features in patients affected by COVID-19 included GGO, consolidation, interlobular septal thickening, adjacent pleura thickening, and air bronchograms.
- The infection most commonly involves the bilateral lungs, especially bilateral lower lobes.
- Similar imaging features are seen in other infections, and the final diagnosis of COVID-19 should still be based on reverse-transcription polymerase chain reaction.

### REFERENCES

- Nizzari M, Thellung S, Corsaro A, et al. Neurodegeneration in Alzheimer disease: role of amyloid precursor protein and presenilin 1 intracellular signaling. *J Toxicol* 2012;2012:187297.
- Huang C, Wang Y, Li X, et al. Clinical features of patients infected with 2019 novel coronavirus in Wuhan, China. *Lancet* 2020;395:497-506.
- Chen N, Zhou M, Dong X, et al. Epidemiological and clinical characteristics of 99 cases of 2019 novel coronavirus pneumonia in Wuhan, China: a descriptive study. *Lancet* 2020;395:507-13.
- Higgins JP, Thompson SG. Quantifying heterogeneity in a meta-analysis. *Stat Med* 2002;21:1539-58.
- Egger M, Davey Smith G, Schneider M, et al. Bias in meta-analysis detected by a simple, graphical test. *BMJ* 1997;315:629-34.
- Ai T, Yang Z, Hou H, et al. Correlation of chest CT and RT-PCR testing in coronavirus disease 2019 (COVID-19) in China: a report of 1014 cases. *Radiology* 2020;200642.

835  
836  
837  
838  
839  
840  
841  
842  
843  
844  
845  
846  
847  
848  
849  
850  
851  
852  
853  
854  
855  
856  
857  
858  
859  
860  
861  
862  
863  
864  
865  
866  
867  
868  
869  
870  
871  
872  
873  
874  
875  
876  
877  
878  
879  
880  
881  
882  
883  
884  
885  
886

Q8

Q9

7. Bernheim A, Mei X, Huang M, et al. Chest CT findings in coronavirus disease-19 (COVID-19): relationship to duration of infection. *Radiology* 2020:200463.
8. Guan WJ, Ni ZY, Hu Y, et al. Clinical characteristics of coronavirus disease 2019 in China. *N Engl J Med* 2020.
9. Pan Y, Guan H, Zhou S, et al. Initial CT findings and temporal changes in patients with the novel coronavirus pneumonia (2019-nCoV): a study of 63 patients in Wuhan, China. *Eur Radiol* 2020.
10. Shi H, Han X, Jiang N, et al. Radiological findings from 81 patients with COVID-19 pneumonia in Wuhan, China: a descriptive study. *Lancet Infect Dis* 2020.
11. Song F, Shi N, Shan F, et al. Emerging coronavirus 2019-nCoV pneumonia. *Radiology* 2020:200274.
12. Wang J, Liu J, Wang Y, et al. [Dynamic changes of chest CT imaging in patients with corona virus disease-19 (COVID-19)]. *Zhejiang Da Xue Xue Bao Yi Xue Ban* 2020;49:0.
13. Wu J, Liu J, Zhao X, et al. Clinical characteristics of imported cases of COVID-19 in Jiangsu Province: a multicenter descriptive study. *Clin Infect Dis* 2020.
14. Wu J, Wu X, Zeng W, et al. Chest CT Findings in patients with corona virus disease 2019 and its relationship with clinical features. *Invest Radiol* 2020.
15. Xu X, Yu C, Qu J, et al. Imaging and clinical features of patients with 2019 novel coronavirus SARS-CoV-2. *Eur J Nucl Med Mol Imaging* 2020.
16. Xu YH, Dong JH, An WM, et al. Clinical and computed tomographic imaging features of novel coronavirus pneumonia caused by SARS-CoV-2. *J Infect* 2020.
17. Zhang JJ, Dong X, Cao YY, et al. Clinical characteristics of 140 patients infected with SARS-CoV-2 in Wuhan, China. *Allergy* 2020.
18. Zhang MQ, Wang XH, Chen YL, et al. [Clinical features of 2019 novel coronavirus pneumonia in the early stage from a fever clinic in Beijing]. *Zhonghua Jie He He Hu Xi Za Zhi* 2020;43:E013.
19. Xie X, Zhong Z, Zhao W, et al. Chest CT for typical 2019-nCoV pneumonia: relationship to negative RT-PCR testing. *Radiology* 2020:200343.
20. Fang Y, Zhang H, Xie J, et al. Sensitivity of chest CT for COVID-19: comparison to RT-PCR. *Radiology* 2020:200432.
21. Chong S, Kim TS, Cho EY. Herpes simplex virus pneumonia: high-resolution CT findings. *Br J Radiol* 2010;83:585-9.
22. Wong KT, Antonio GE, Hui DS, et al. Thin-section CT of severe acute respiratory syndrome: evaluation of 73 patients exposed to or with the disease. *Radiology* 2003;228:395-400.
23. Das KM, Lee EY, Al Jawder SE, et al. Acute Middle East respiratory syndrome coronavirus: temporal lung changes observed on the chest radiographs of 55 patients. *AJR Am J Roentgenol* 2015;205:W267-74.
24. Malainou C, Herold S. [Influenza]. *Internist (Berl)* 2019;60:1127-35.
25. de Wit E, van Doremalen N, Falzarano D, et al. SARS and MERS: recent insights into emerging coronaviruses. *Nat Rev Microbiol* 2016;14:523-34.
26. Hui DSC, Zumla A. Severe acute respiratory syndrome: historical, epidemiologic, and clinical features. *Infect Dis Clin North Am* 2019;33:869-89.
27. Zu ZY, Jiang MD, Xu PP, et al. Coronavirus disease 2019 (COVID-19): a perspective from China. *Radiology* 2020:200490.
28. Kooraki S, Hosseiny M, Myers L, et al. Coronavirus (COVID-19) outbreak: what the department of radiology should know. *J Am Coll Radiol* 2020.
29. Ooi GC, Daqing M. SARS: radiological features. *Respirology* 2003;8(Suppl):S15-9.
30. Das KM, Lee EY, Langer RD, et al. Middle East respiratory syndrome coronavirus: what does a radiologist need to know? *AJR Am J Roentgenol* 2016;206:1193-201.

887  
888  
889  
890  
891  
892  
893  
894  
895  
896  
897  
898  
899  
900  
901  
902  
903  
904  
905  
906  
907  
908  
909  
910  
911  
912  
913  
914  
915  
916  
917  
918  
919  
920  
921  
922  
923  
924  
925  
926  
927  
928  
929  
930  
931  
932  
933  
934  
935  
936  
937  
938

UNCORRECTED